Single electron ionization of multishell atoms: dynamic screening and post–prior discrepancies in the CDW-EIS model

2013 J. Phys. B: At. Mol. Opt. Phys. 46 145201

(http://iopscience.iop.org/0953-4075/46/14/145201)

J. Phys. B: At. Mol. Opt. Phys. **46** (2013) 145201 (6pp) doi:10.1088/0953-4075/46/14/145201

Single electron ionization of multishell atoms: dynamic screening and post–prior discrepancies in the CDW-EIS model

J M Monti[1], **O A Fojón**[1], **J Hanssen**[2] **and R D Rivarola**[1]

[1] Laboratorio de Colisiones Atómicas, Facultad de Ciencias Exactas, Ingeniería y Agrimensura, and Instituto de Física Rosario (CONICET-UNR) Universidad Nacional de Rosario, Avenida Pellegrini 250, 2000 Rosario, Argentina

[2] Laboratoire de Physique Moléculaire et des Collisions, ICPMB (FR CNRS 2843), Institut de Physique, Université de Lorraine, 1 rue Arago, F-57078 Metz Cedex 3, France

E-mail: monti@ifir-conicet.gov.ar

Received 20 February 2013, in final form 22 May 2013
Published 21 June 2013
Online at stacks.iop.org/JPhysB/46/145201

Abstract

A complete formulation of the *post*-version of the continuum distorted wave-eikonal initial state (CDW-EIS) model is used to investigate single ionization of multishell atoms by fast bare proton beams. The influence of the non-ionized electrons on the dynamic evolution is studied for each of the different shells of the targets. Its inclusion was made by means of the parametric Green–Sellin–Zachor potential. In this way, it is shown that discrepancies between the *prior*- and *post*-versions of the CDW-EIS model are avoided for any *nl* states of the systems studied here. The present analysis is supported by comparisons with existing experimental electron emission spectra.

(Some figures may appear in colour only in the online journal)

1. Introduction

Electron ionization of atomic and molecular targets by the impact of ion beams has been a subject of main interest since long ago [1]. Single ionization of atomic targets by swift bare-ion impact was first studied in terms of perturbative Born series, but several issues have risen, among them divergences arising from the existence of disconnected diagrams [2] and from the presence of intermediate elastic channels [3]. The use of the distorted wave formalism, and thus of corresponding distorted wave series, avoids these undesirable behaviours. These series are also proposed to accelerate their convergence, so that it can be reached only by employing the corresponding few first terms [4–7]. Several distorted wave models have been developed, and much of this theoretical work can be found in textbooks [1, 8]. Among them, we can highlight the continuum distorted wave (CDW; [9]) and the CDW-eikonal initial state (CDW-EIS; [10]) ones. They were originally formulated for the case of monoelectronic targets, but these models can be extended for single ionization of multielectronic targets employing the general formulation introduced by Fainstein *et al* [11]. In that formulation, the multielectronic system is reduced to an effective monoelectronic one, assuming that the non-ionized electrons (the passive ones) remain frozen in their initial orbitals. For CDW-EIS (CDW), in the entry channel the initial-bound state was described by means of a Hartree–Fock wavefunction distorted by a multiplicative eikonal phase (continuum factor) representing the *active* electron in a continuum state of the projectile field. In the exit channel, for both approximations, the continuum of the *active* electron was described by the product of a plane wave and two continuum factors, each one of them associated with the residual target and projectile fields. Thus, the passive electrons were supposed to affect mainly the projectile trajectory while the active one was assumed to move independently of them. The CDW-EIS model has been applied with success to a wide variety of collisional systems and its validity has been established for the range of intermediate to high collision energies (see [1, 12]).

To facilitate the calculation of transition matrix elements, and the corresponding cross sections, effective Coulomb potentials were chosen to represent the interaction between

the active and the passive electrons in the exit channel. As a consequence of the simple consideration of an effective Coulomb continuum of the residual target, a post–prior discrepancy was obtained when cross sections were computed using the respective *post*- and *prior*-versions of the scattering matrix elements [13, 14].

Gulyás *et al* [15, 16] addressed this problem using a different approach to describe the active electron wavefunctions into a three-body approximation. One-electron bound and continuum target eigenstates were considered using the same Hartree–Fock–Slater residual target potential. These wavefunctions were obtained by solving numerically the corresponding target Schrödinger equation. With this choice, post–prior discrepancies were eliminated but hard numerical computation of cross sections was involved.

Recently, Monti *et al* [17, 18] showed for the case of single ionization of He by proton impact that the inclusion in the *post*-version of the CDW-EIS approximation of an additional potential, that was neglected in all previous calculations when an effective Coulomb target potential was adopted, leads to the vanishing of the post–prior discrepancies. This potential, calculated within the Hartree–Fock approximation [17, 18], takes account of the dynamic screening (at intermediate distances) produced by the passive electron cloud on the ejected electron in the exit channel.

In this work, following these ideas, the investigation has now been extended to the case of multishell atomic targets. The dynamic screening for each particular orbital is considered by using a two-parameter Green–Sellin–Zachor (GSZ) potential [19–21]. The use of this potential provides a simpler analytical expression for the transition matrix element and facilitates the calculations of the cross sections. Also, the comparison between the results obtained with this *post*-version and the *prior*-one using the Roothaan–Hartree–Fock (RHF) functions to describe the target initial state could give an estimate of the range of applicability of the two-parameter GSZ potential with an increasing number of electrons of the target. As this potential only has two parameters, it may have some limitations describing in detail the potential produced by a multishell atom.

In the following section, we briefly review the *prior*- and *post*-versions of the CDW-EIS model and the inclusion of the dynamic screening in the *post*-version through the use of a GSZ parametric potential.

Atomic units will be used in the following except when stated otherwise.

2. Theory

The CDW-EIS approximation was introduced by Crothers and McCann [10] to study single ionization of H by bare-ion impact. Previous studies had shown that the CDW model failed at intermediate impact energies due to the lack of normalization of the initial state. The CDW-EIS solved this problem presenting, in general, a very good agreement with the experimental data for the total cross sections (TCS).

Fainstein *et al* [11] (see also [1, 12] and references therein) showed that for single ionization of bare-ion impact, within the independent electron model, a multielectronic system can be reduced to a monoelectronic one, assuming that the rest of the electrons remain frozen in their initial orbitals. It is thus supposed that the passive electrons can only relax post-collisionally. Therefore, this approximation will be valid at sufficiently high collision energies. Therefore, within this independent electron model and considering that there is just one active electron, the multielectronic Hamiltonian can be reduced to

$$H_{\rm el} = -\tfrac{1}{2}\nabla^2 + V_T(\mathbf{x}) + V_P(\mathbf{s}) + V_s(\mathbf{R}) \tag{1}$$

where $\mathbf{x}(\mathbf{s})$ is the active electron coordinate in the target (projectile) reference frame, $V_T(\mathbf{x})$ is the effective one-electron target potential, $V_P(\mathbf{s}) = -Z_P/s$ is the interaction between the bare projectile and the active electron and $V_s(\mathbf{R})$ is the interaction of the projectile with the target nucleus and the passive electrons. This last potential depends only on the internuclear coordinate $\mathbf{R}$ and thus, within the straight-line version of the impact-parameter approximation, gives rise to a phase factor which does not affect the electron dynamics [11]. In the following, we therefore drop this term.

The CDW-EIS approximation is the first-order approximation of a distorted wave series in which the initial and final distorted waves are proposed as

$$\chi_i^+(\mathbf{x}, t) = \Phi_i(\mathbf{x}, t)\, \mathcal{L}_i^+(\mathbf{s}), \tag{2}$$

$$\chi_f^-(\mathbf{x}, t) = \Phi_f(\mathbf{x}, t)\, \mathcal{L}_f^-(\mathbf{s}), \tag{3}$$

respectively. In (2) and (3), $\Phi_i(\mathbf{x}, t) = \phi_i(\mathbf{x}) \exp(\mathrm{i}\varepsilon_i t)$ and $\Phi_f(\mathbf{x}, t) = \phi_f(\mathbf{x}) \exp(\mathrm{i}\varepsilon_f t)$ are the initial-bound and final-continuum state solutions of the time-dependent Schrödinger equation, in the exit channel with the effective Coulomb target potential $V_T(\mathbf{x})$. Also, ε_i (ε_f) is the electron energy in the initial (final) state. The initial-bound state of the target is considered as an RHF wavefunction (see [22] and the appendix), and the final-continuum one is written as

$$\phi_f(\mathbf{x}) = \frac{1}{(2\pi)^{3/2}} \exp(\mathrm{i}\mathbf{k}\cdot\mathbf{x}) \times N^*(\lambda)\, {}_1F_1[-\mathrm{i}\lambda, 1, -\mathrm{i}\,(kx + \mathbf{k}\cdot\mathbf{x})], \tag{4}$$

with energy $\varepsilon_f = k^2/2$, $\mathbf{k}$ being the ejected electron momentum in the target reference frame, $N(a) = \exp(\pi a/2)\Gamma(1 + \mathrm{i}a)$ (with Γ being Euler's Gamma function) is the normalization factor of the ${}_1F_1$ hypergeometric function, and $\lambda = \tilde{Z}_T/k$ with $\tilde{Z}_T$ an effective or net target charge to be chosen.

The initial distortion is proposed as

$$\mathcal{L}_i^+(\mathbf{s}) = \exp[-\mathrm{i}\nu \ln(vs + \mathbf{v}\cdot\mathbf{s})], \tag{5}$$

whereas the final distortion is chosen as

$$\mathcal{L}_f^-(\mathbf{s}) = N^*(\zeta)\, {}_1F_1[-\mathrm{i}\zeta; 1; -\mathrm{i}\,(ps - \mathbf{p}\cdot\mathbf{s})] \tag{6}$$

where $\mathbf{v}$ is the projectile velocity, $\nu = Z_P/v$, $\zeta = Z_P/p$, $\mathbf{p} = \mathbf{k} - \mathbf{v}$ the ejected electron momentum in the projectile reference frame.

Both the initial (2) and final (3) wavefunctions with the distortions given by (5) and (6), satisfy the correct asymptotic conditions at $t \to -\infty$ and $t, x, s \to +\infty$, respectively.

Table 1. Parameters d and K of the GSZ potential for the different targets considered, extracted from [20].

Target	d (au)	$K = dH$ (au)
Ne	0.558	2.71
Ar	1.045	3.50

The *prior*-version of the transition amplitude for the CDW-EIS approximation can be written as

$$\mathcal{A}_{if}^{-}(\rho) = -\mathrm{i}\int_{-\infty}^{+\infty} \mathrm{d}t\, \langle \chi_f^{-} | (W_i | \chi_i^{+}) \rangle \tag{7}$$

provided now that the initial distorted wavefunction χ_i^{+} does not contribute to the transition amplitude as $t \to +\infty$. In (7), W_i is the well-known EIS perturbative operator:

$$W_i\, \chi_i^{+} = \Phi_i(\mathbf{x}, t)\left[\tfrac{1}{2}\nabla_{\mathbf{s}}^2 \mathcal{L}_i^{+}(\mathbf{s}) + \nabla_{\mathbf{x}} \ln \phi_i(\mathbf{x}) \cdot \nabla_{\mathbf{s}} \mathcal{L}_i^{+}(\mathbf{s})\right]. \tag{8}$$

Proceeding as in [17, 18], the *post*-version of the transition amplitude can be written as

$$\mathcal{A}_{if}^{+}(\rho) = -\mathrm{i}\int_{-\infty}^{+\infty} \mathrm{d}t\, [\langle \chi_f^{-} | (W_f^{\dagger} + \tilde{V}_T)] | \chi_i^{+} \rangle\,, \tag{9}$$

provided that the final distorted wavefunction χ_f^{-} does not contribute to the transition amplitude as $t \to -\infty$. In (9), W_f is the widely used CDW perturbative operator

$$W_f^{-}\, \chi_f^{-} = \Phi_f(\mathbf{x}, t)[\nabla_{\mathbf{x}} \ln \phi_f(\mathbf{x}) \cdot \nabla_{\mathbf{s}} \mathcal{L}_f^{-}(\mathbf{s})], \tag{10}$$

and the additional potential

$$\tilde{V}_T(\mathbf{x}) = -(Z_T - \tilde{Z}_T)/x + V_{ap}(\mathbf{x}), \tag{11}$$

$V_{ap}(\mathbf{x})$ being the interaction between the active electron and the passive ones. This $\tilde{V}_T$ potential is the one usually excluded in the usual *post*-version of the CDW-EIS model.

Choosing $\tilde{Z}_T = n_i\sqrt{-2\varepsilon_i}$ (see [23]), or $\tilde{Z}_T = Z_T - N$ in (11) (and correspondingly in $\phi_f(\mathbf{x})$), N being the number of passive electrons of the target, one obtains either the effective or the asymptotic form of the *post*-version of the scattering amplitude, respectively.

In this case, we consider $\tilde{V}_T$ in terms of a GSZ analytical parametric potential, and rewrite (11), resulting in

$$\tilde{V}_T(\mathbf{x}) = -\frac{(q - \tilde{Z}_T)}{x} - \frac{(Z_T - q)}{x}\Omega(x) \tag{12}$$

with

$$\Omega(x) = [H(\mathrm{e}^{x/d} - 1) + 1]^{-1}, \tag{13}$$

where $q = Z_T - N$, and H and d are parameters depending on Z_T and N. The parameters used for each target are shown in table 1.

3. Results and discussions

Double differential cross sections (DDCS) for single ionization of Ar atoms by impact of protons, as a function of the electron energy at fixed emission angles, are presented in figures 1 and 2, for collision energies of 300 keV and 1 MeV, respectively. Theoretical DDCS are compared with the existing experimental data [24]. The DDCS were calculated using the

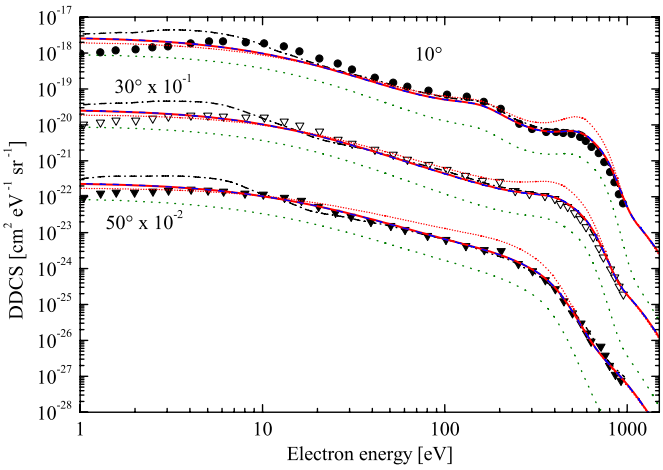

Figure 1. Doubly differential cross section (DDCS) for single ionization in collisions of 300 keV H^+ on Ar targets as a function of the electron energy for 10°, 30° and 50° fixed emission angle. Theory: *full line*, *complete post*-CDW-EIS calculations with effective charges; *short dotted line*, *post*-CDW-EIS calculations with effective charges; *dotted line*, *post*-CDW-EIS calculations with asymptotic charges; *dashed line*, *prior*-CDW-EIS calculations with effective charges; *chain line*, CDW-EIS calculations from Gulyás *et al* [27]. Experiment: *symbols*, Rudd *et al* [24].

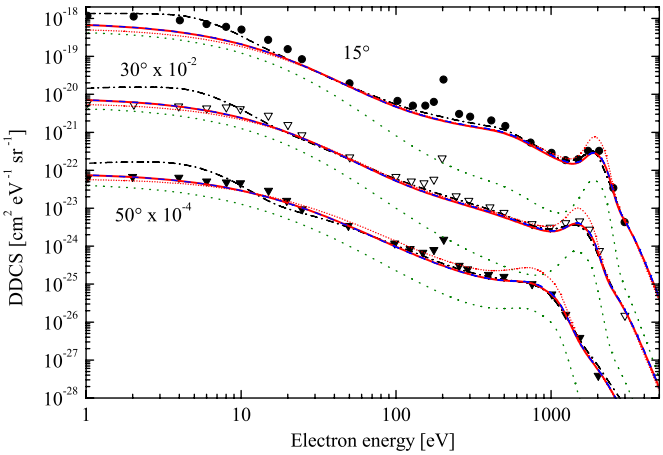

Figure 2. Same as figure 1 but for 1 MeV collision energy and 15°, 30° and 50° fixed emission angle. Theory: *full line*, *complete post*-CDW-EIS calculations with effective charges; *short dotted line*, *post*-CDW-EIS calculations with effective charges; *dotted line*, *post*-CDW-EIS calculations with asymptotic charges; *dashed line*, *prior*-CDW-EIS calculations with effective charges; *chain line*, CDW-EIS calculations from Gulyás *et al* [27]. Experiment: *symbols*, Rudd *et al* [24].

CDW-EIS *prior*- and *post*-choosing effective or asymptotic charges in the residual target final-continuum function.

According to the independent particle model given by Kirchner *et al* [25] (see also [26]), these DDCS could also be interpreted as net (inclusive) cross sections, where at least one electron of the atomic target is ionized.

For both impact energies, the agreement of DDCS obtained with the *prior*-version and the *complete post*-version (where the potential $\tilde{V}_T$ was included) is so close that they cannot be distinguished in the figures. Theoretical

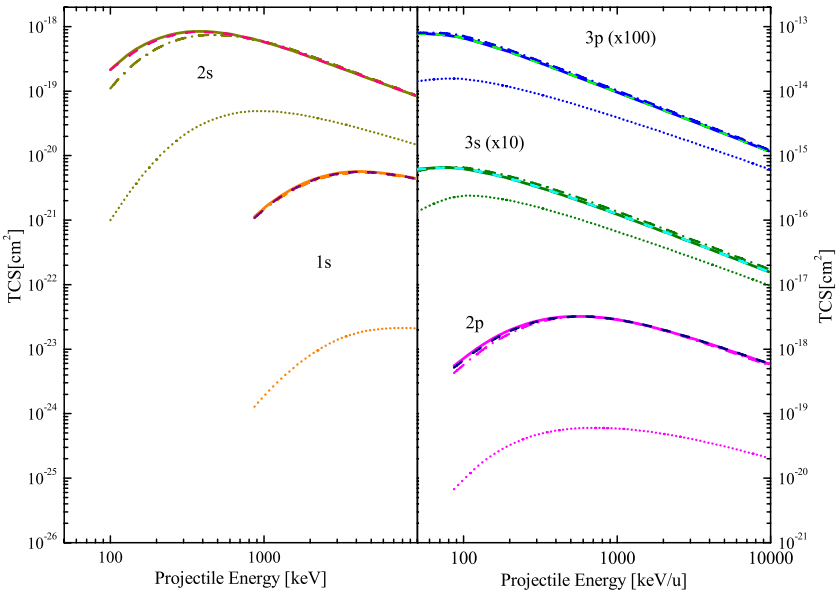

Figure 3. Total cross section (TCS) for single ionization in collisions of H^+ on Ar targets as a function of the collision energy. Theory: · · · · · ·, *post*-CDW-EIS calculations with asymptotic charges; — · —, *post*-CDW-EIS calculations with effective charges; ————, *complete post*-CDW-EIS calculations with effective charges; – – – –, *prior*-CDW-EIS calculations with effective charges.

calculations give a very good description of measurements. However, some differences between results obtained with the *prior*-version and the usual *post*-version (which excludes the contribution of the $\tilde{V}_T$ term) are found, particularly in the binary encounter peak region, where the usual *post*-version overestimates the experimental data. This shows that the appropriate consideration of the $\tilde{V}_T$ potential in the *post*-version calculations avoids the presence of post–prior discrepancies.

DDCS calculated employing the asymptotic (net) target charge in the usual *post*-version are also presented. With this choice, the short-range part of the interaction between the active and the passive electrons in the exit channel is neglected. Therefore, their comparison with the complete CDW-EIS results put in evidence the main role played by the dynamic screening on the emission of the active electron. The better agreement between the *complete post*-version and the usual *post*-version with effective target charges is due to the fact that, with this choice, the dynamic screening is partially included.

The *prior*-result and the *complete post*-result are also in good accordance with CDW-EIS results from [27]. The latter were calculated considering a numeric residual target continuum function in the exit channel, and therefore taking into account all orders of the *dynamic screening*. Some discrepancies are however observed at low electron energies for which the DDCS are higher than those calculated using the *prior*-result or *complete post*-result with an effective Coulomb continuum. This different behaviour could be associated with the fact that electrons emitted with low velocities are more sensitive to the target potential and so to a more adequate description of the corresponding continuum wavefunction. However, unexpectedly, for most of the cases presented here, these numerical-continuum DDCS appear as overestimating the experimental data.

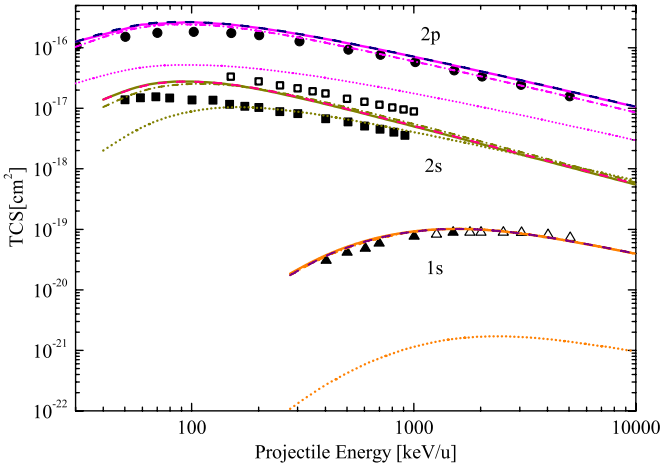

Figure 4. TCS for single ionization in collisions of H^+ on Ne targets as a function of the collision energy. Theory: · · · · · ·, *post*-CDW-EIS calculations with asymptotic charges; — · —, *post*-CDW-EIS calculations with effective charges; ————, *complete post*-CDW-EIS calculations with effective charges; – – – –, *prior*-CDW-EIS calculations with effective charges. Experiments: △, Cocke *et al* [28]; ▲, Rødbro *et al* [29]; ■, Eckhardt and Schartner [31]; □, Hippler and Schartner [30]; •, total Ne ionization from Rudd *et al* [33].

In figures 3 and 4, we present TCS as a function of the collision energy for single ionization of Ar and Ne atoms by proton impact, respectively. The contributions to the TCS from the different atomic orbitals are discriminated. For the cases considered here, the *prior*-version and *complete post*-version give similar results for all the atomic shells of the targets. It is an indication of the feasibility of using the GSZ potential for ionization of any shells in the complete CDW-EIS model. There are some minor differences between the previous results and those corresponding to the usual *post*-version using

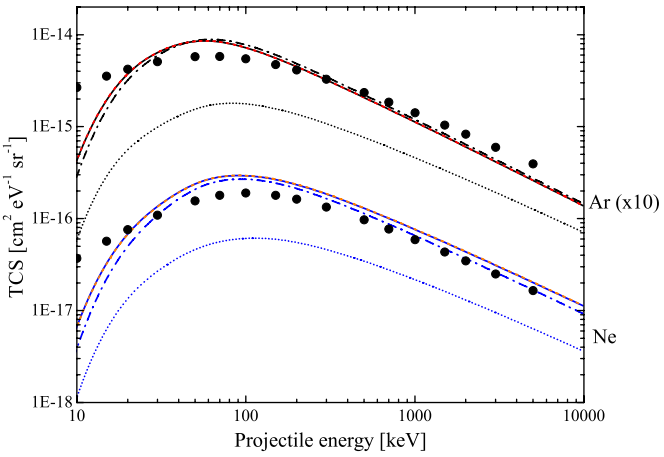

Figure 5. TCS for single ionization in collisions of H^+ on Ar and Ne targets as a function of the collision energy. Theory: · · · · · ·, *post*-CDW-EIS calculations with asymptotic charges; — · —, *post*-CDW-EIS calculations with effective charges; ————, *complete post*-CDW-EIS calculations with effective charges; – – – –, *prior*-CDW-EIS calculations with effective charges. Experiments: •, total Ar and Ne ionization from Rudd *et al* [33].

effective charges at small collision energies. This difference diminishes as outer shells are considered. The comparison with calculations employing the usual *post*-approximation with asymptotic target charge in the exit channel allows us again to estimate the importance of dynamic screening contributions on TCS. For inner orbitals, this contribution may be larger than two orders of magnitude at high impact velocities (see for example ionization of the K-shell of Ar in figure 3). The influence of the dynamic screening is found to be reduced as the principal quantum number increases, for s- as well as for p-states. This can be understood from the fact that the Coulomb target factor implicitly takes account of the region from which the electron in its initial orbital is ejected, and thus the use of an asymptotic target charge result is inadequate for the inner shells. Meanwhile for the outermost shells, the dynamic screening is almost completely considered when taking an effective Coulomb target potential. As can be seen in figure 4, the agreement between experimental results and CDW-EIS ones in its *prior*-version and *complete post*-version is in general very good except perhaps for the 2s orbital. For this case, we present experimental results from [30] and [31]. Both sets were obtained in quite the same way by using photon spectroscopy techniques, and they are practically the same except that the latter one was enlarged with new measurements. However, the relative efficiency of the optical detection system for these new measurements was redetermined. Consequently, the result of this redetermination is that published results from [30] have to be reduced by a factor of 2.6 as stated in [32]. Our predictions lie between both mentioned sets. However, the agreement seems to be better with experiments from [30].

In figure 5, we show TCS for Ar and Ne ionization, summing the contributions from all different orbitals. Once again, an overall agreement is observed between experiments and CDW-EIS cross sections.

4. Conclusions

A *complete post*-version of the CDW-EIS approximation is used to describe single ionization of multishell atomic targets by proton impact. Contributions coming from the active electron–residual target interaction in the final channel are considered in terms of a GSZ parametric potential. For the Ne and Ar targets considered in this work, the differential and total spectra for electron emission obtained by including this interaction in the *post*-version of the model are in close agreement with the ones calculated within its *prior*-version, so that post–prior discrepancies vanish. This behaviour is found for any of the atomic shells considered. Present results can be thus considered as an extension of those previously reported in [18] for K-shell electrons in the case of the ionization of He atoms by proton impact. This agreement gives an indication that the GSZ potential gives an appropriate description of the interaction between the active electron and the residual target and can be thus used with confidence when the *post*-version of the CDW-EIS is employed to describe electron emission from different target orbitals, at least for targets having up to 18 electrons.

Contributions on DDCS and TCS of the dynamic screening produced by passive electrons on the evolution of the ejected one are evaluated for ionization from the different shells of the targets studied here. As it could be expected, its influence appears to be more important for the inner shells and diminishes as outer shells are considered.

Acknowledgments

The authors thank the Consejo Nacional de Investigaciones Científicas y Técnicas and the Agencia Nacional de Promoción Científica y Tecnológica, both from Argentina, for partial financial support of the work through the projects PIP 1026 and PICT 2011-2145.

Appendix. Calculation of the initial-bound state ϕ_i

The active electron initial-bound state is described within the Roothaan–Hartree–Fock approximation, being thus represented by a linear combination of Slater-type functions:

$$\phi_i = \sum_j C_j \, \chi_{p_j \lambda_j \alpha_j}. \tag{A.1}$$

The $\chi_{p\lambda\alpha}$ functions are Slater-type orbitals, given by

$$\chi_{p\lambda\pm\alpha}(\mathbf{r}) = R_{p\lambda}(r) Y_\lambda^{\pm\alpha}(\hat{\mathbf{r}}), \tag{A.2}$$

where

$$R_{p\lambda}(r) = \frac{(2Z_{p\lambda})^{p+1/2}}{\sqrt{(2p)!}} \, r^{p-1} \, \exp(-Z_{p\lambda} r), \tag{A.3}$$

and $Y_\lambda^{\pm\alpha}$ is a spherical harmonic ($\alpha \geqslant 0$).

A generating function $\varphi(\mathbf{r})$

$$\varphi(\mathbf{r}) = \exp(-\mathrm{i}\,\boldsymbol{\mu} \cdot \mathbf{r} - \beta\, r) \tag{A.4}$$

can be used to obtain the different $\chi_{p\lambda\alpha}$ functions in (A.1), by the action of an operator $\hat{D}_{p\lambda\alpha}$, so that

$$\chi_{p\lambda\alpha}(\mathbf{r}) = \hat{D}_{p\lambda\alpha} \varphi(\mathbf{r})\big|_{\boldsymbol{\mu}=0,\, \beta=Z_{p\lambda}}. \tag{A.5}$$

In (A.5),

$$\hat{D}_{p\lambda\alpha} = C_{p\lambda\alpha}\,\hat{D}^{(1)}_{p\lambda}\,\hat{D}^{(2)}_{\lambda\alpha}\,\hat{D}^{(3)}_{\pm\alpha}, \tag{A.6}$$

with

$$C_{p\lambda\alpha} = \frac{(-1)^{p-1}\,(2Z_{p\lambda})^{p+1/2}}{(2\mathrm{i})^{\lambda}\,\lambda!}\sqrt{\frac{(2\lambda+1)}{4\pi}\frac{(\lambda-\alpha)!}{(2p)!\,(\lambda+\alpha)!}}, \tag{A.7}$$

$$\hat{D}^{(1)}_{p\lambda} = \left(\frac{\partial}{\partial\beta}\right)^{p-\lambda-1}, \tag{A.8}$$

$$\hat{D}^{(2)}_{\lambda\alpha} = \sum_{k=0}^{\left[\frac{\lambda-\alpha}{2}\right]}\binom{\lambda}{k}\frac{(2\lambda-2k)!}{(\lambda-\alpha-2k)!}\left(\frac{\partial}{\partial\beta}\right)^{2k}\left(\mathrm{i}\frac{\partial}{\partial\mu_z}\right)^{\lambda-\alpha-2k}, \tag{A.9}$$

and

$$\hat{D}^{(3)}_{\pm\alpha} = (-1)^{\frac{\lambda\pm1}{2}\alpha}\left(\frac{\partial}{\partial\mu_x}\pm\mathrm{i}\frac{\partial}{\partial\mu_y}\right)^{\alpha} \tag{A.10}$$

$$= (-1)^{\frac{\lambda\pm1}{2}\alpha}\sum_{s=0}^{\alpha}\binom{\alpha}{s}(\pm\mathrm{i})^{\alpha-s}\left(\frac{\partial}{\partial\mu_x}\right)^{\alpha}\left(\frac{\partial}{\partial\mu_y}\right)^{\alpha-s}. \tag{A.11}$$

Also in (A.9), $\left[\frac{\lambda-\alpha}{2}\right]$ indicates the integer part of the fraction considered.

References

[1] Stolterfoht N, DuBois R D and Rivarola R D 1997 *Electron Emission in Heavy Ion–Atom Collisions* (Berlin: Springer)
[2] Joachain C J 1975 *Quantum Collision Theory* (Amsterdam: North-Holland)
[3] Dewangan D P and Eichler J 1987 *Comment. At. Mol. Phys.* **21** 1
[4] Francis N C and Watson K M 1954 *Phys. Rev.* **93** 313
[5] Greider K R and Dodd L R 1966 *Phys. Rev.* **146** 671
[6] Dodd L R and Greider K R 1966 *Phys. Rev.* **146** 675
[7] Gayet R 1972 *J. Phys. B: At. Mol. Phys.* **5** 483
[8] Bransden B H and McDowell M R C 1992 *Charge Exchange and the Theory of Ion–Atom Collisions* (Oxford: Clarendon)
[9] Belkić Dž 1978 *J. Phys. B: At. Mol. Phys.* **11** 3529
[10] Crothers D S F and McCann J F 1983 *J. Phys. B: At. Mol. Phys.* **16** 3229
[11] Fainstein P D, Ponce V H and Rivarola R D 1988 *J. Phys. B: At. Mol. Opt. Phys.* **21** 287
[12] Fainstein P D, Ponce V H and Rivarola R D 1991 *J. Phys. B: At. Mol. Opt. Phys.* **24** 3091
[13] Ciappina M F, Cravero W R and Garibotti C R 2003 *J. Phys. B: At. Mol. Opt. Phys.* **36** 3775
[14] Ciappina M F and Cravero W R 2006 *J. Phys. B: At. Mol. Opt. Phys.* **39** 1091
[15] Gulyás L, Fainstein P D and Salin A 1995 *J. Phys. B: At. Mol. Opt. Phys.* **28** 245
[16] Gulyás L and Fainstein P D 1998 *J. Phys. B: At. Mol. Opt. Phys.* **31** 3297
[17] Monti J M, Fojón O A, Hanssen J and Rivarola R D 2010 *J. At. Mol. Opt. Phys.* **2010** 128473
[18] Monti J M, Fojón O A, Hanssen J and Rivarola R D 2010 *J. Phys. B: At. Mol. Opt. Phys.* **43** 205203
[19] Green A E S, Sellin D L and Zachor A S 1969 *Phys. Rev.* **184** 1
[20] Szydlik P P and Green A E S 1973 *Phys. Rev.* A **9** 1885
[21] Garvey R H, Jackman C H and Green A E S 1975 *Phys. Rev.* **12** 1144
[22] Clementi E and Roetti C 1974 *At. Data Nucl. Data Tables* **14** 177
[23] Belkić Dž, Gayet R and Salin A 1979 *Phys. Rep.* **56** 279
[24] Rudd M E, Toburen L H and Stolterfoht N 1979 *At. Data Nucl. Data Tables* **23** 405
[25] Kirchner T, Gulyás L, Moshammer R, Schulz M and Ullrich J 2002 *Phys. Rev.* A **65** 042727
[26] Rivarola R D, Galassi M, Fainstein P D and Champion C 2013 *Advances in Quantum Chemistry* vol 65 chapter 9 (Amsterdam: Elsevier) p 231
[27] Gulyás L, Fainstein P D and Salin A 1995 *J. Phys. B: At. Mol. Opt. Phys.* **28** 245
[28] Cocke C L, Gardner R K, Curnutte B, Bratton T and Saylor T K 1977 *Phys. Rev.* A **16** 2248
[29] Rødbro M, Horsdal Pedersen E, Cocke C L and Macdonald J R 1979 *Phys. Rev.* A **19** 1936
[30] Hippler R and Schartner K-H 1974 *J. Phys. B: At. Mol. Phys.* **7** 1167
[31] Eckhardt M and Schartner K-H 1983 *Z. Phys.* A **312** 321
[32] Beyer H F, Hippler R, Schartner K-H and Albat R 1979 *Z. Phys.* A **289** 239
[33] Rudd M E, Kim Y K, Madison D H and Gallagher J W 1985 *Rev. Mod. Phys.* **57** 965